

Feasibility of applying dual injection DCE-MRI technique in liver study

Amy Watkins¹, Ka-Loh Li¹, Xiaoping Zhu¹, and Alan Jackson¹

¹Wolfson Molecular Imaging Centre, University of Manchester, Manchester, United Kingdom

Target audience: Investigators using DCE-MRI in liver cancer research.

Purpose: Mapping kinetic parameters from dynamic contrast-enhanced MRI (DCE-MRI) traditionally requires compromise in terms of spatial resolution, temporal resolution, and volume coverage. A dual injection dynamic contrast-enhanced (DICE) MRI approach has been applied for brain tumor study to improve both the spatial resolution and the accuracy of kinetic mapping¹. In this study we present limit the results of applying the DICE method in liver.

Methods: DCE-MRI data were acquired from two healthy volunteers. Each of them received two scans with a 14-day interval. Four consecutive 3D fast gradient recalled echo acquisitions (TR/TE = 2.5/0.699 ms) with an array of flip angles, 2°, 8°, 15°, and 20° were acquired with an image matrix of 112x112x22 to allow calculation of native longitudinal relaxation rate (R10) maps. A high temporal resolution (HTR) DCE-MRI series (n = 300) with a time interval (Δt) of 1.28 s was acquired and a prebolus (dose 0.02 mmol /kg body weight) of contrast agent (CA) was administered after the 20th dynamic frame. High spatial resolution (HSR) data sets, with a matrix size of 320x320x70 and voxel size of 0.94x0.94x2 mm³, were then collected including four consecutive 3D fast gradient recalled echo acquisitions (TR/TE = 3.7/0.93 ms) with flip angles of (2°, 8°, 15°, and 20°) and a DCE-MRI series (60 time frames with Δt = 10.7 s). A standard dose of dotarem (0.1 mmol/kg) was administered after the 5th dynamic frame. All volumetric MR images were obtained in coronal plane. Arterial input function (AIF) were measured in the aorta from both DCE datasets. The extended Tofts version of the Kety model was used for kinetic analysis² to produce maps of transfer coefficient (K^{trans}), fractional volume of blood plasma (v_p), extravascular-extracellular space (v_e) and an AIF offset time (τ_a).

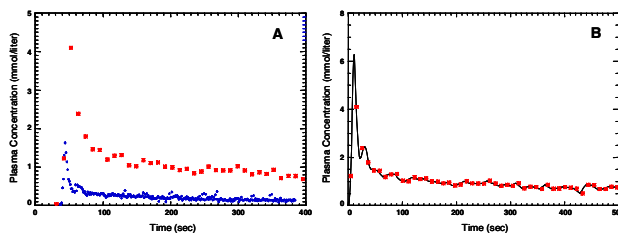


Fig. 1: Reconstruction of AIF from dual injection data. **A:** $C_p(t)$ curves measured from the prebolus DCE (blue diamond) and the main dose DCE (red asterisk), plotted with aligned bolus arrival time. **B:** Reconstructed AIF (solid black line) with low temporal resolution AIF from main dose (red asterisk).

published literature². HTR prebolus data can provide more accurate bolus arrival time.

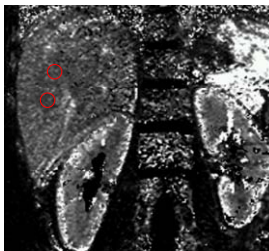


Fig. 2: HSR K^{trans} map in a coronal plane, with two ROIs (Red) drawn on liver.

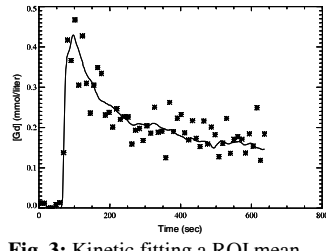


Fig. 3: Kinetic fitting a ROI mean liver tissue [Gd]-time curve from the main dose scan using HTR AIF reconstructed from prebolous scan.

Results: The prebolus AIF was reconstructed with a method described elsewhere¹ to form the early part of the HTR AIF for kinetic analysis of the HSR DCE MRI data. Fig. 1 displays the plasma concentration-time curves, $C_p(t)$, measured from aorta in volunteer 1 (fig. 1A) and the reconstructed HTR AIF (fig. 1B).

For each of the four HTR and four HSR datasets, a region of interest (ROI) was manually defined in a center slice of the liver, avoiding any major vessels. The ROI size was 24 ± 4 in HTR data, 179 ± 18 in HSR data. Table 1 lists the ROI mean \pm SD of longitudinal relaxation time (T1) values, which are consistent with published literatures^{3,4}.

Fig. 2 shows a HSR K^{trans} map from visit 2 of volunteer 2 imaged during normal breathing. ROIs were manually drawn on liver. The ROI mean/median kinetic parameter values were: $K^{trans} = 0.38/0.37 \text{ min}^{-1}$; $v_p = 0.0047/0.0039$; and $v_e = 0.26/0.24$. Fig. 3 shows fitting the Tofts-Kety model to ROI-averaged liver tissue [Gd]-time course from the HSR data of volunteer 1, using the reconstructed HTR AIF (Fig. 1B). The various parameter obtained were: $K^{trans} = 0.47 \text{ min}^{-1}$; $v_p = 0.00066$; $v_e = 0.22$ and $\tau_a = 10.1 \text{ s}$. These parameter values are close to liver kinetic parameters in literature^{3,4}.

Fig. 4 shows a BAT map from HTR data of volunteer 1.

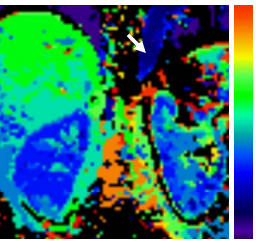


Fig. 4: Spatial distribution in BAT measured from HTR data. Note that aorta (white arrow) has a BAT of 39.1 sec.

Discussion: This feasibility study demonstrates that combining information content from HTR and HSR data in liver produces a high quality HTR AIF providing improvement in the accuracy of HSR kinetic parameter maps. The low temporal sampling rate of the HSR sequence allows full liver coverage with a voxel size of 2 mm³. The low dose HTR data can also be advantageously used for kinetic analysis⁵, e.g., providing more accurate BAT maps. The limitation of this work is failure to correct for motion effects. Reducing movement-induced artifacts will be the key step for our future work in applying the DICE technique in liver cancer study.

Table 1: Mean \pm SD ROI T1 values

T1 (ms)	Visit 1		Visit 2	
	HT	HS	HT	HS
Subj 1	657 \pm 47	641 \pm 143	579 \pm 26	620 \pm 116
Subj 2	619 \pm 35	628 \pm 86	607 \pm 41	620 \pm 102

References:

- 1) Li KL, Buonaccorsi G, Thompson G, et al. An improved coverage and spatial resolution--using dual injection dynamic contrast-enhanced (ICE-DICE) MRI: a novel dynamic contrast-enhanced technique for cerebral tumors. *Magn Reson Med*. 2012;68(2):452-462.
- 2) Banerji A, Naish JH, Watson Y, et al. DCE-MRI model selection for investigating disruption of microvascular function in livers with metastatic disease. *J Magn Reson Imaging*. 2012;35(1):196-203.
- 3) de Bazelaire CM, Duhamel GD, Rofsky NM, et al. MR imaging relaxation times of abdominal and pelvic tissues measured in vivo at 3.0 T: preliminary results. *Radiology* 2004;230(3):652-659.
- 4) Thomsen C, Christoffersen P, Henriksen O, et al. Prolonged T1 in patients with liver cirrhosis: an in vivo MRI study. *Magnetic resonance imaging* 1990;8(5):599-604.
- 5) Baxter S, Wang ZJ, Joe BN, et al. Timing bolus dynamic contrast-enhanced (DCE) MRI assessment of hepatic perfusion: Initial experience. *J Magn Reson Imaging* 2009;29(6):1317-1322.